View metadata, citation and similar papers at core.ac.uk
brought to you by CORE
provided by University of Queensland eSpace

Balanced Interhemispheric Cortical Activity Is Required for Correct Targeting of the Corpus Callosum

Rodrigo Suárez, Laura R. Fenlon, Roger Marek, Lilach Avitan, Pankaj Sah, Geoffrey J. Goodhill, Linda J. Richards

Summary

Bilateral integration of sensory and associative brain processing is achieved by precise connections between homologous regions in the two hemispheres via the corpus callosum. These connections form postnatally, and unilateral deprivation of sensory or spontaneous cortical activity during a critical period severely disrupts callosal wiring. However, little is known about how this early activity affects precise circuit formation. Here, using in utero electroporation of reporter genes, optogenetic constructs, and direct disruption of activity in callosal neurons combined with whisker ablations, we show that balanced interhemispheric activity, and not simply intact cortical activity in either hemisphere, is required for functional callosal targeting. Moreover, bilateral ablation of whiskers in symmetric or asymmetric configurations shows that spatially symmetric interhemispheric activity is required for appropriate callosal targeting. Our findings reveal a principle governing axon targeting, where spatially balanced activity between regions is required to establish their appropriate connectivity.

Introduction

The development of functional brain circuits involves the sequential regulation of early stages of neuronal differentiation and axonal growth, as well as guidance by morphogenic and guidance molecular cues, followed by later stages of axonal arborization and synaptic refinement, mediated by spontaneous and sensory-evoked electrical activity (Katz and Shatz, 1996, Goldberg et al., 2002, Spitzer, 2006 and Mire et al., 2012). Early neuronal activity critically affects brain development in three main ways. First, the endogenous pattern of activity in a given neuron affects its axonal growth rate and responses to external cues (Cohan and Kater, 1986, Fields et al., 1990, Ming et al., 2001, Goldberg et al., 2002, Tang et al., 2003, Hanson and Landmesser, 2004 and Mire et al., 2012). Second, the relative patterns of activity between individual axons projecting to the same targets can determine competitive interactions between them, ultimately affecting wiring patterns, as has been well documented in the visual system (Casagrande and Condo, 1988, Penn et al., 1998, Huberman et al., 2006, Ben Fredj et al., 2010, Zhang et al., 2012 and Furman et al., 2013). Finally, manipulation of the activity of either pre- or postsynaptic neurons can also affect axonal wiring patterns (Zhang et al., 1998 and Yamada et al., 2010). Such is the case in the development of interhemispheric connections, where the targeting of callosal axons is impaired when activity is disrupted either in the cell bodies of projecting axons or in their contralateral targets (Mizuno et al., 2007, Wang et al., 2007 and Mizuno et al., 2010). However, it is not clear whether particular aspects of activity are independently required in both projecting neurons and their targets or if, instead, a balance of activity between regions is sufficient for precise interhemispheric wiring.

Here, we investigate the role of early activity in the development of interhemispheric cortical connections of the corpus callosum. This commissure is the largest fiber tract in the eutherian brain, allowing bilateral integration of lateralized brain processes (Gazzaniga, 2000, Shuler et al., 2001 and Shuler et al., 2002) and interhemispheric transfer of sensory input (Ebner and Myers, 1962 and Calford and Tweedale, 1990). Callosal axons connect mainly homotopic (Yorke and Caviness, 1975, Krubitzer et al., 1998, Catania and Kaas, 2001 and Zhou et al., 2013) but also heterotopic cortical regions (Boyd et al., 1971 and Kretz and Rager, 1990), including projections arising from cells in primary sensory areas of one hemisphere that end in dense terminals at the border between the corresponding primary and secondary sensory areas of the contralateral hemisphere (Innocenti and Fiore, 1976, Wise and Jones, 1976 and Ivy and Killackey, 1981). Formation of these callosal projections occurs at postnatal stages in rodents and is prevented by unilateral disruptions of sensory input (Innocenti and Frost, 1979, Olavarria et al., 1987 and Koralek and Killackey, 1990) or excitability of cortical neurons via overexpression of Kir2.1, a hyperpolarizing inward-rectifying potassium channel (Mizuno et al., 2007, Wang et al., 2007 and Mizuno et al., 2010). It has previously been shown that both sensory deprivation of the whisker pad (Yang et al., 2009) and overexpression of Kir2.1 in cortical neurons (Yamada et al., 2010) affect the electrical activity of the cortex, which suggests that their effect on the development of callosal projections are due to altered cortical activity. However, exactly how activity affects interhemispheric targeting is not known. As the corpus callosum connects homotopic regions of both hemispheres, each receiving similarly organized thalamic afferents, we hypothesized that similar cortical activity between hemispheres guides the establishment of correct interhemispheric connections.

To address this, we examined the formation of callosal projections in the somatosensory cortex. In mammals, unlike the visual system, somatosensory pathways are entirely decussated, making it possible to examine the effects of specifically altering peripherally or cortically driven activity in one or both hemispheres. We show that, whereas unilateral disruptions of either peripherally or cortically driven activity impair somatosensory callosal targeting, bilateral manipulations result in a rescue of projections. To examine this further, we altered the spatial arrangement of functional whiskers on each side of the face and found that only bilaterally symmetric patterns of sensory input result in a rescue of callosal projections. We conclude that balanced neuronal activity between interhemispheric homotopic regions is necessary during development for normal callosal targeting.

Results

Normal Callosal Targeting Requires Bilaterally Balanced Thalamocortical Input

To specifically label callosal neurons and their axonal projections in mice, the fluorescent tag enhanced yellow fluorescent protein (eYFP) was expressed in layer 2/3 (L2/3) of primary somatosensory cortex (S1) by in utero electroporation at embryonic day (E) 15.5 (Figures 1A and 1B). These callosal axons cross the midline and arborize profusely at the border between S1 and the secondary somatosensory cortex (S2) by the end of the first postnatal week,

when they achieve an adult-like innervation pattern (Wise and Jones, 1978, Ivy and Killackey, 1981 and Wang et al., 2007) (Figure 1A; Figure S1 available online). At postnatal day (P) 3, we disrupted the sensory inputs to S1 by cauterizing the follicles of the mystacial whiskers on one or both sides of the face and examined the patterns of callosal innervation at P10 (Figure 1B). Whisker cauterization at this stage prevents the formation of thalamocortical barrels in layer 4 (L4) of S1 (Figures 1C–1E), which have a topographic one-to-one spatial relationship with whiskers on the contralateral side of the face (Woolsey and Van der Loos 1970). Whisker cauterization also prevents regrowth of whiskers (Figures S1K–S1M) and ensures full disruption of barrels, which are less affected by other methods of sensory deprivation such as whisker plucking (Fox, 1992). Unilateral ablation of sensory afferents to the electroporated hemisphere ($n = 6$) resulted in a disruption of contralateral callosal projections to all cortical layers of the S1/S2 border region as compared to controls ($n = 7$; $p < 0.01$; Figures 1F and 1G; Figures S1A and S1B). Similarly, sensory deprivation of the nonelectroporated (target) hemisphere ($n = 8$) also resulted in a disrupted S1/S2 projection compared to control (layer 1 [L1], $p < 0.01$; L2/3, $p < 0.01$; Figures S1C–S1E). This result is consistent with previous findings in the visual system, in which callosal projections are affected when activity is disrupted in either the cell bodies of callosal neurons or in their contralateral targets, with cell body disruptions showing a more severe phenotype (Mizuno et al., 2010). Therefore, for all further analysis, we manipulated inputs to the cell bodies to ensure a maximal baseline of callosal disruption. Previous studies reporting disruption of the S1/S2 callosal projection under unilateral ablations of peripheral or thalamic afferences to S1 have suggested that a reduced input to the cortex may explain this effect (Koralek and Killackey, 1990). This proposal predicts that cauterization of the whiskers on both sides of the face would result in a similar or even greater disruption of callosal targeting. It is surprising, however, that we observed the opposite effect: bilaterally cauterized animals ($n = 8$) showed a significant rescue of callosal projections to S1/S2 when compared to animals with unilateral cauterization (L1, $p < 0.05$; L2/3, $p < 0.01$; Figures 1F–1I; quantification of fluorescence normalized by the underlying white matter [f/fwm] is expressed on the right and in subsequent figures as a relative percentage of control). This effect was also observed in adult (P50) animals that received unilateral ($n = 7$), bilateral ($n = 4$), or no ($n = 6$) cauterization at P3 (L2/3, $p < 0.05$; Figures S1F–S1J). This demonstrates that this effect is not transient but rather persists into adulthood and may underlie enduring differences in connectivity and function. Taken together, these findings indicate that the total magnitude of sensory input may be less important for callosal targeting to S1/S2 than its interhemispheric balance.

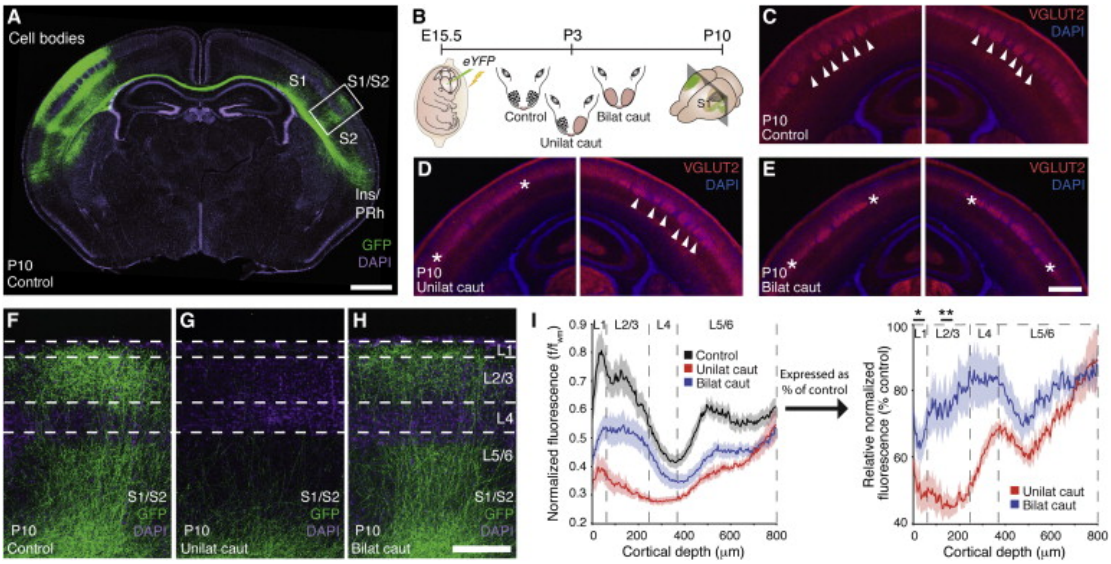

Figure 1.

Unilateral Cauterization Disrupts S1/S2 Callosal Projection Formation, whereas Bilateral Cauterization Results in a Partial Rescue

(A) Coronal section of a control P10 mouse brain after electroporating eYFP in utero at E15 in S1 (cell bodies) showing contralateral projections to the S1/S2 border (rectangle) and the Ins/PRh. Scale bar, 1 mm.

(B) Schematic of the experimental procedure.

(C–E) Vesicular glutamate transporter 2 (VGlut2) staining of (C) control, (D) unilaterally cauterized, and (E) bilaterally cauterized animals, showing the presence (arrowheads) or disruption (asterisks) of barrels at P10. Scale bar, 500 μm.

(F–H) Representative examples of the S1/S2 callosal projection of (F) control (n = 7), (G) unilaterally cauterized (n = 6), and (H) bilaterally cauterized (n = 8) animals. Scale bar, 200 μm.

(I) Quantification of fluorescence intensity across layers normalized by fluorescence of the underlying white matter (f/fwm) in the S1/S2 region shows a decrease in fluorescence for unilaterally cauterized animals and a partial rescue for bilaterally cauterized animals. Data are presented as absolute traces (left) and after transformation to relative percentage of controls (right) in order to standardize comparisons and avoid unnecessary data repetition. Each value comprising the blue and red traces on the left were divided by the corresponding value of the control (black) trace to produce the graph on the right (mean ± SEM). Subsequent fluorescence intensity data will be presented as a relative percentage of control unless stated otherwise. Student's t test: ∗p < 0.05, ∗∗p < 0.01.

See also Figure S1.

Figure options

Activity Dependence of Somatosensory Callosal Targeting Is Region Specific

Previous studies assessing the role of early activity on callosal wiring have focused on targets to the S1/S2 region, but whether other contralateral targets of callosal neurons from L2/3 of S1 (Figure 1A) show similar effects has not been investigated. Thus, we next set out to examine the effect of differential cauterization manipulations on the sparse callosal projections to the contralateral S1 and a dense projection to the insular/perirhinal cortex (Ins/PRh; Figure 2A). We found that neither unilateral (n = 6) nor bilateral (n = 8) cauterization manipulations altered the callosal projection to S1 compared to control (n = 7; Figures 2B–2E; Figure S2A). Similarly, the Ins/PRh projection was not affected by unilateral (n = 6) or bilateral (n = 8) cauterization manipulations compared to control (n = 8; Figures 2F–2I; Figure S2B). This provides the first indication, to our knowledge, of different rules affecting the development of discrete callosal projections from the same population of cells.

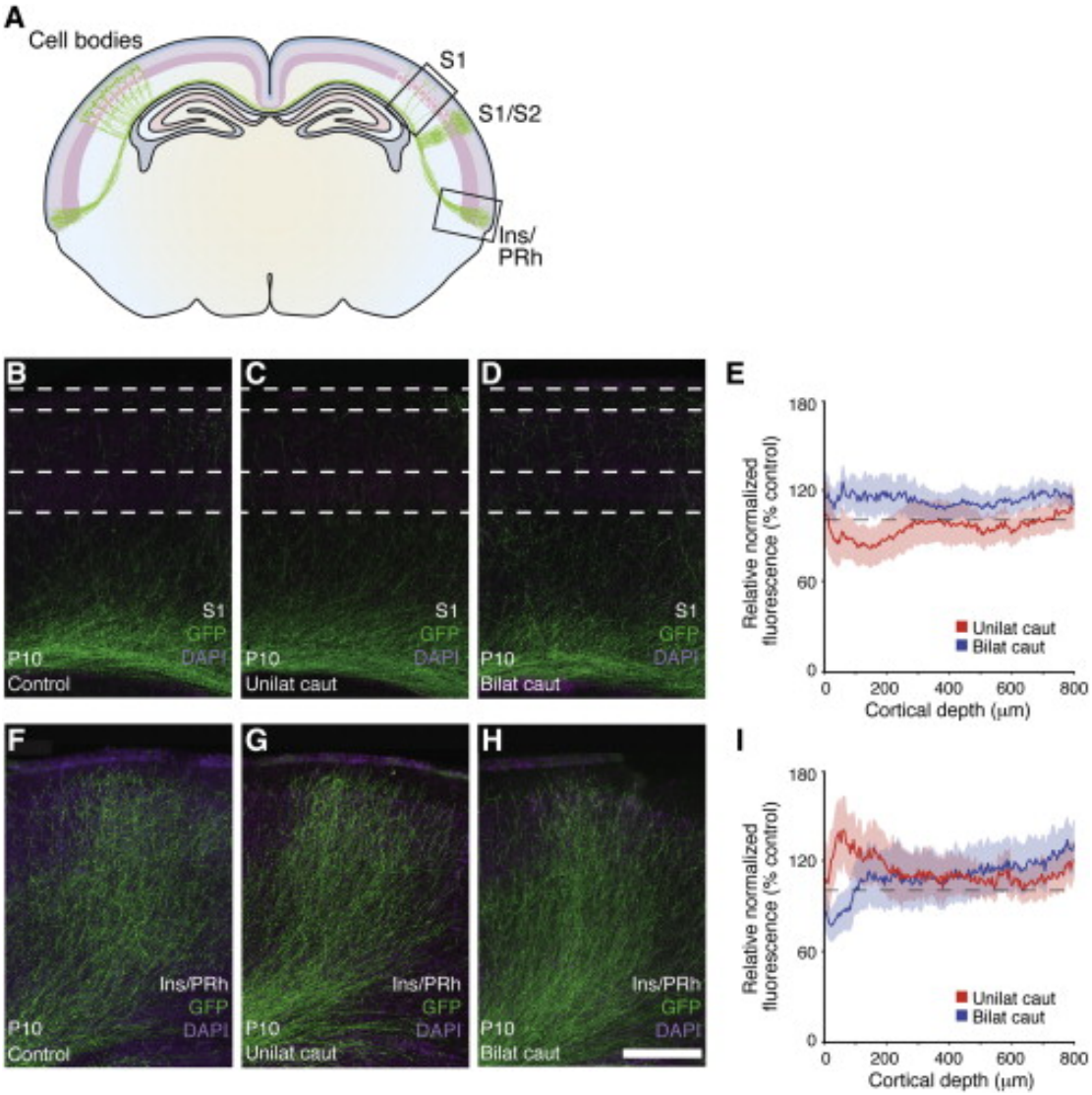

Figure 2.

Whisker Cauterization Does Not Affect Callosal Projections to the Contralateral S1 and Ins/Prh Regions

(A) Schematic of the locations of callosal projections shown in (B)–(H).

(B–D) Representative examples of S1 projections in (B) control, (C) unilateral, and (D) bilateral cauterization conditions.

(E) Quantification of normalized fluorescence of callosal projections to S1 as a relative percentage of control (Unilat caut, n = 6; Bilat caut, n = 8; Control, n = 7) shows no significant differences between conditions (mean ± SEM).

(F–H) Representative examples of callosal projections to the Ins/PRh region for (F) control, (G) unilateral, and (H) bilateral cauterization conditions.

(I) Normalized fluorescence intensity analysis for callosal projections to the Ins/PRh region (Unilat caut, n = 6; Bilat caut, n = 8; Control, n = 8) also showed no significant differences between conditions (mean ± SEM). Scale bar, 300 μm.

See also Figure S2.
Figure options

Disrupted S1/S2 Callosal Projections under Unilateral Whisker Cauterization Are Functionally Rescued under Bilateral Whisker Cauterization

Next, we sought to evaluate whether the S1/S2 callosal projection in bilaterally cauterized animals was functionally rescued by comparing the presynaptic and postsynaptic integrity of the contralateral S1/S2 innervation between treatments. To quantify presynaptic terminals, we performed in utero coelectroporation of the presynaptic marker synaptophysin-GFP and the membrane-directed fluorophore Myr-tdTomato (Harwell et al., 2012) at E15.5 in callosal neurons of S1, and determined the number of green fluorescent puncta in individual axons of the contralateral S1/S2 region at P10. Interestingly, we found no difference between conditions, suggesting that although unilaterally cauterized animals had fewer axons terminating in L2/3 than either control or bilaterally cauterized animals, the number of synapses per unit of axonal length was not affected by the manipulations (Figures 3A–3D). The integrity of postsynaptic targets was then assessed using an optogenetic approach (Petreanu et al., 2007), which revealed that functional connectivity of callosal axons was fully rescued in bilaterally cauterized animals. We expressed channelrhodopsin-2 in S1 callosal neurons by in utero electroporation at E15.5. Whole-cell recordings were obtained from L2/3 neurons of the contralateral S1/S2 region, and callosal afferents to these cells were photostimulated using whole-field 470 nm light pulses (5 ms) (Figure 3E). Recordings were made from three types of neurons: intrinsically bursting and regular spiking pyramidal neurons and fast spiking interneurons (Figure S3). For quantitative analysis between whisker cauterization treatments, the two types of pyramidal neurons were considered collectively, as their electrical properties and magnitude of callosal input did not differ (Figures S3B–S3D). We also filled select neurons

with biocytin after recordings and confirmed the morphological identity of pyramidal and interneuron cell types (Figures 3F and 3G). As compared to controls (n = 7), significantly fewer L2/3 pyramidal neurons in the S1/S2 region of unilaterally cauterized animals (n = 8) were activated by photostimulation of callosal terminals (innervation rate, $p < 0.001$; Figure 3H). In contrast, bilaterally cauterized animals (n = 7) had a significantly higher innervation rate of pyramidal neurons than unilaterally cauterized animals ($p < 0.05$; Figure 3H). A similar pattern was found for interneurons, where unilaterally cauterized animals (n = 5) had a smaller innervation rate than control animals (n = 6; $p < 0.05$), while bilaterally cauterized animals (n = 4) did not differ from controls (Figure 3I). Next, we compared the postsynaptic responses of cells activated by photostimulation of callosal terminals. We found that pyramidal neurons of unilaterally cauterized animals (n = 8) have significantly smaller amplitude of the excitatory postsynaptic current (EPSC) than controls (n = 7; $p < 0.05$), while bilaterally cauterized animals showed a significant rescue (n = 7; $p < 0.01$; Figure 3J). These findings indicate that, while unilaterally cauterized animals have a reduction in the number of callosal inputs that each neuron receives compared to control, this is rescued in bilaterally cauterized animals. Because of the small number of callosally innervated L2/3 interneurons in the unilaterally cauterized condition (2 of 16 cells examined in seven animals), we were not able to perform a comparison of EPSCs between interneurons. Nevertheless, to assess whether the effects were exclusively due to changes in callosal connectivity and not to altered inputs from other presynaptic sources, we compared the spontaneous excitatory events in L2/3 pyramidal neurons between conditions. We found no significant differences in either the frequency or amplitude of the miniature EPSCs recorded in the absence of stimulation in control (n = 7), unilaterally cauterized (n = 8), or bilaterally cauterized (n = 7) animals (Figures 3K and 3L), demonstrating that the postsynaptic differences observed between the cauterization treatments on photostimulation of callosal fibers are due to functional changes in callosal connectivity. Together, these results show that functionally active callosal connections are formed even in the absence of sensory input and that a bilaterally balanced contribution of input is crucial to functional brain wiring.

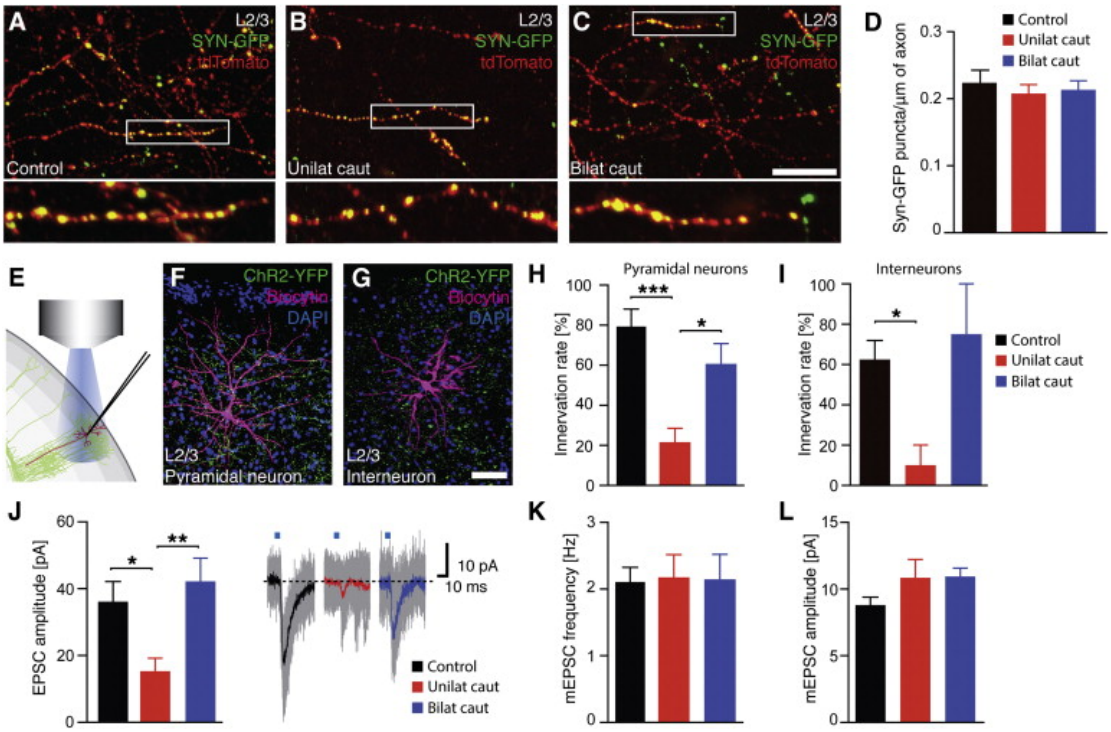

Figure 3.

Functional Integrity of Pre- and Postsynaptic Components of the S1/S2 Callosal Projection in Control and Cauterized Animals

(A–C) Representative examples of tdTomato-expressing axons (red) with presynaptic terminals expressing synaptophysin-GFP (green) in L2/3 of the S1/S2 callosal projection of (A) control (n = 8), (B) unilaterally cauterized (n = 9), and (C) bilaterally cauterized (n = 9) animals. Scale bar, 25 µm.

(D) Quantification of presynaptic terminals (green puncta) per micrometer of tdTomato-positive axon in each condition showed no differences between conditions (mean ± SEM).

(E) Schematic of L2/3 neuron (magenta) recordings following photostimulation of S1/S2 callosal terminals (green) expressing channelrhodopsin-2.

(F and G) Representative examples of (F) a L2/3 pyramidal neuron and (G) an interneuron filled with biocytin after recordings. Scale bar, 50 µm.

(H and I) Synaptic innervation rate (percentage of recorded cells that were activated by callosal photostimulation) of (H) pyramidal neurons (n = 7, control; n = 8, unilaterally cauterized; n = 7, bilaterally cauterized animals) and (I) interneurons (n = 6, control; n = 5, unilaterally cauterized; n = 4, bilaterally cauterized animals) in L2/3 of the S1/S2 region (mean ± SEM).

(J) EPSC amplitude of pyramidal neurons in L2/3 of S1/S2 for each condition (n = 7, control; n = 8, unilaterally cauterized; n = 7, bilaterally cauterized animals), showing a significant decrease and rescue in unilaterally and

bilaterally cauterized animals (mean ± SEM). Representative traces of EPSCs evoked by 5 ms photostimulation of callosal terminals (blue bars) are shown on the right.

(K and L) Average (K) frequency and (L) amplitude of spontaneous miniature EPSCs (mEPSCs) of pyramidal neurons in the absence of photostimulation did not differ between conditions (n = 7, control; n = 7, unilaterally cauterized; n = 7, bilaterally cauterized animals; mean ± SEM). Mann-Whitney U test: $*p < 0.05$, $**p < 0.01$, $***p < 0.001$.

See also Figure S3.
Figure options

Normal Callosal Targeting Requires a Balance of Endogenous Activity between Hemispheres

The formation of functional callosal projections in bilaterally cauterized animals could be exclusively due to matching thalamic input to the cortex or could reflect a more general requirement of balanced cortical activity between hemispheres. To investigate this, we compared callosal projections after disrupting electrical activity directly in L2/3 callosal neurons in one or both hemispheres while leaving the sensory periphery intact. We reduced neuronal excitability by coelectroporating in utero the inward rectifier potassium channel Kir2.1 and eYFP in one hemisphere alone or followed by coelectroporation of the contralateral S1 with Kir2.1 and the red fluorescent tag DsRed (Figure 4A). Using two different fluorophores allowed us to select animals with bilaterally homologous electroporation sites within S1. Neurons expressing Kir2.1 (n = 9) were less excitable, showing a more hyperpolarized resting membrane potential ($p < 0.001$; Figure 4B), a longer first-spike latency ($p < 0.01$; Figure 4C), a lower input resistance ($p < 0.001$; Figure 4D), and a characteristic inward-rectifying current-voltage relationship (Figure 4E), as compared to control cells (n = 7). Notably, the integrity of thalamocortical barrels in L4 was not affected by this treatment, as revealed by VGlut2 immunohistochemistry (Figure 4F, arrowheads). Previous studies have shown that unilateral expression of Kir2.1 in callosal neurons disrupts contralateral projections to the border of the primary and secondary cortices, leading to the proposal that intrinsic neuronal activity is critically required for callosal wiring (Mizuno et al., 2007, Wang et al., 2007 and Mizuno et al., 2010). We confirmed those findings in our experiments (Figure 4G). However, similar to our previous results, disrupting the activity of L2/3 callosal neurons in both hemispheres (n = 7) resulted in a significant rescue of callosal projections to L2/3 of the S1/S2 border, as compared to unilateral Kir2.1 expression (n = 9; percentage of control, L2/3, $p < 0.05$; Figures 4G–4I; Figures S4A and S4B). The other contralateral callosal projections were not affected by unilateral Kir2.1 expression (S1, n = 9; Ins/PRh, n = 5) or bilateral Kir2.1 expression (S1, n = 7; Ins/PRh, n = 5), as compared to control (S1, n = 7; Ins/PRh, n = 8; Figures 4J–4O and Figures S4C and S4D), again showing that this effect is region specific and that expression of Kir2.1 does not result in a generalized disruption of axonal growth. The presence of barrels in L4, regardless of Kir2.1 expression, demonstrates that innervation of thalamocortical axons is not

sufficient for callosal targeting and excludes the possibility of differential axonal competition between thalamic and callosal terminals. Together, these results suggest that the requirement of an early postnatal interhemispheric balance for callosal targeting to S1/S2 can either be sensory or cortically driven.

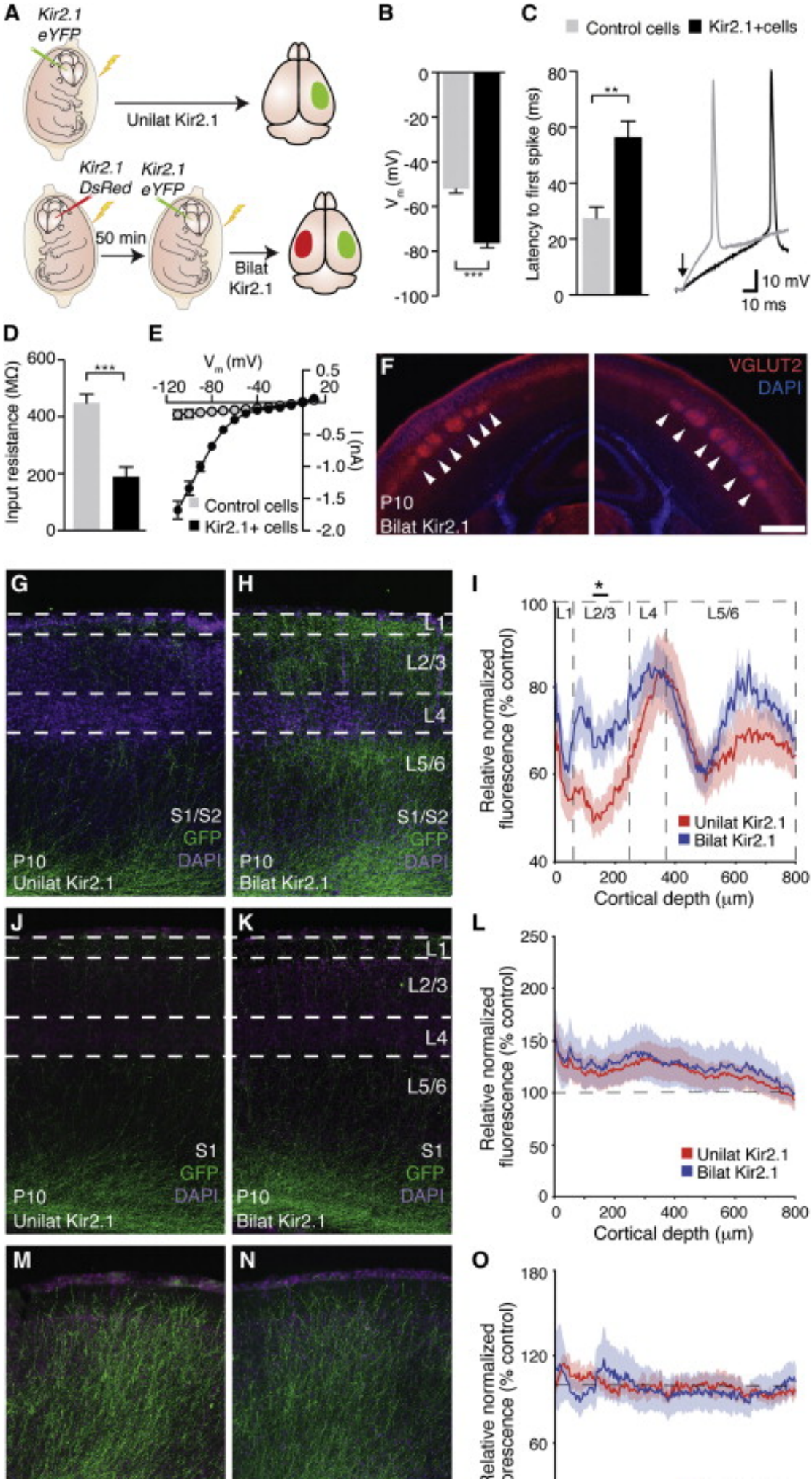
A
Kir2.1
eYFP
Unilat Kir2.1
Kir2.1
DsRed
Kir2.1
eYFP
50 min
Bilat
Kir2.1
B
C
Control cells
Kir2.1+cells
Latency to first spike (ms)
10 mV
10 ms
D
Input resistance (MΩ)
E
Control cells
Kir2.1+ cells
F
VGLUT2
DAPI
P10
Bilat Kir2.1
G
H
L1
L2/3
L4
L5/6
S1/S2
GFP
DAPI
P10
Unilat Kir2.1
P10
Bilat Kir2.1
I
Relative normalized fluorescence (% control)
Unilat Kir2.1
Bilat Kir2.1
Cortical depth (μm)
J
K
S1
L
M
N
O

Figure 4.

Direct Manipulation of Cortically Driven Activity Recapitulates the Unilateral and Bilateral Effects of Sensory Disruptions

(A) Schematics of Kir2.1 overexpression. Bilateral electroporations were performed at least 50 min apart to avoid interventricular transfer of plasmids.

(B–E) Whole-cell recordings of callosal neurons overexpressing Kir2.1 (n = 9, black) and controls (n = 7, gray), recorded from the same animals (n = 3), reveal significant differences in (B) the resting membrane potential, (C) latency of first spike to stimulation (arrow, right traces), (D) input resistance, and (E) current-voltage relationship, demonstrating that Kir2.1 overexpression effectively reduced excitability of transfected neurons (mean ± SEM).

(F) VGlut2 staining (red) shows the presence of intact barrels (arrowheads) when Kir2.1 is expressed in L2/3 cortical cells. Scale bar, 500 μm.

(G–O) Representative examples and quantification of normalized fluorescence intensity across layers as relative percentage of controls revealed significant differences of the callosal projections to S1/S2 (G, unilateral, n = 9; H, bilateral, n = 7; I, n = 7, control) but not to S1 (J, unilateral, n = 9; K, bilateral, n = 7; L, control, n = 7), or to Ins/PRh (M, unilateral, n = 5; N, bilateral, n = 5; O, control, n = 8; mean ± SEM). Student's t test: $*p < 0.05$, $**p < 0.01$, $***p < 0.001$. Scale bars, 200 μm in (G) and (H) and 300 μm in (J)–(N).

See also Figure S4.
Figure options

Bilateral Spatial Symmetry of Somatosensory Input Is Required for Callosal Targeting

Our results thus far have shown that a balance of either sensory input or cortical excitability is required for callosal S1/S2 targeting. However, whether a broad balance of cortical activity is sufficient for callosal targeting to S1/S2 or, instead, a spatially precise interhemispheric matching of inputs is required is not known. During the first postnatal week of rats, oscillatory waves of the local field potential propagate spatially across cortical areas (Garaschuk et al., 2000, Khazipov and Luhmann, 2006, Minlebaev et al., 2011 and Khazipov et al., 2013) and become increasingly synchronized between hemispheres in a point-to-point symmetric manner (Yang et al., 2009). Given that the topographical arrangement of the barrel subfield of S1 is symmetric between hemispheres, we assessed whether interhemispheric symmetry of sensory input is required for normal callosal targeting. We compared the effects of cauterizing a similar number of whiskers in a symmetric versus an asymmetric manner on each side of the face at P3 (Figure 5A). These treatments resulted in the disruption of the corresponding barrels contralateral to the lesion sites (Figures 4B–4D). Notably, symmetric bilateral cauterization of the upper (n = 7) or lower (n = 6) rows of whiskers did not alter the position or fluorescence intensity of the respective

callosal S1/S2 projection (Figures 5C–5E, empty arrowheads; Figures S5A and S5B); thus, we pooled these conditions for further analysis. We next examined the difference between asymmetric and symmetric manipulations and found that, while bilaterally asymmetric (n = 8) whisker cauterizations produced a disrupted S1/S2 callosal projection as compared to controls (n = 7; L1, L2/3, and layer L5/6, $p < 0.01$; Figure 5F and Figures S5C and S5D), bilaterally symmetric cauterizations (n = 13) resulted in a significant rescue of S1/S2 callosal axons in all cortical layers except L4, as compared with asymmetric treatments (percentage of control, $p < 0.01$; Figures 5F–5H and Figures S5C and S5D). Thus, our results demonstrate that bilateral symmetry of cortical input during the critical period is required for the normal formation of callosal connections to the S1/S2 border.

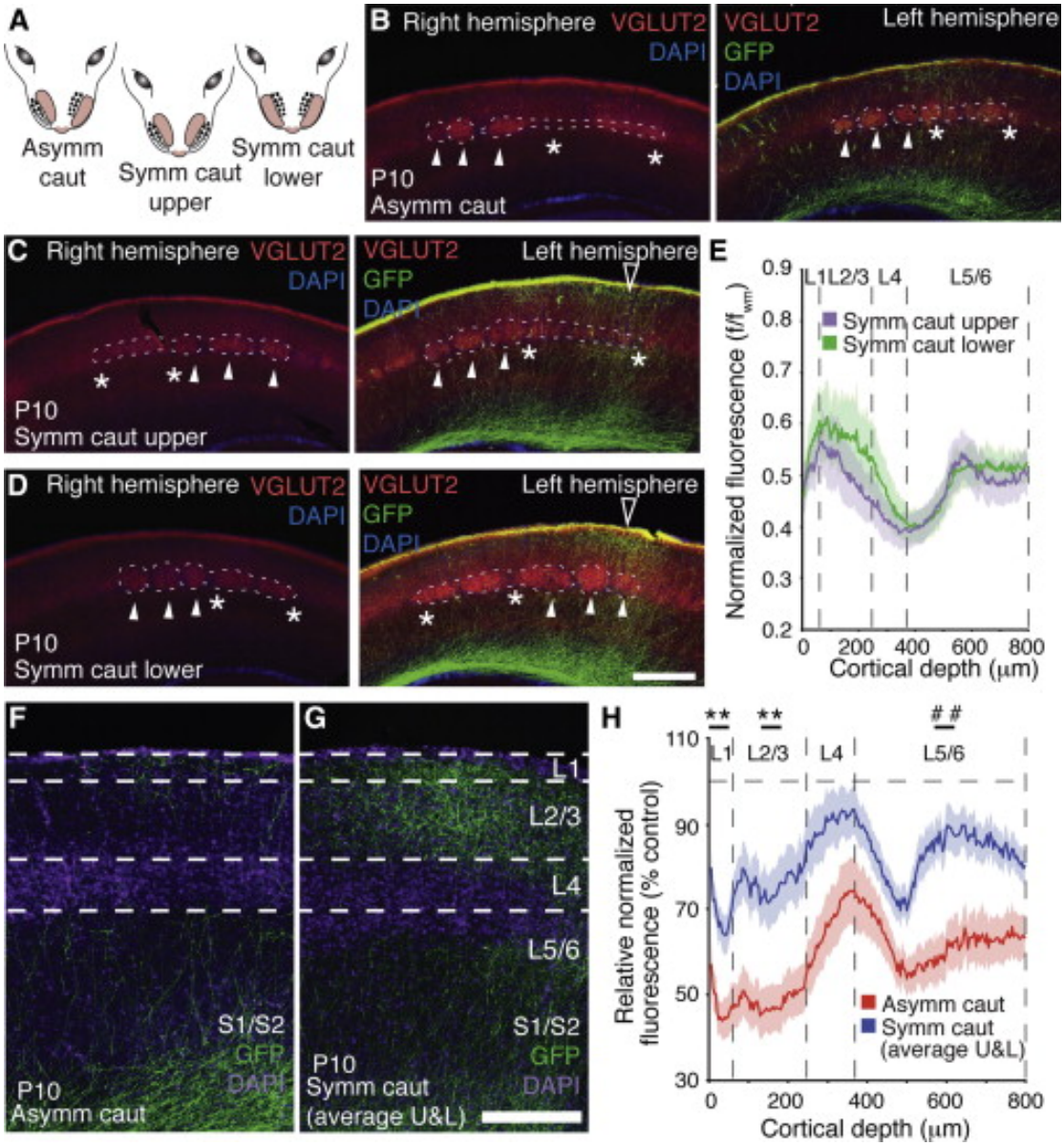

Figure 5.

Spatial Symmetry Is Required for S1/S2 Callosal Projection Formation in Partial Bilateral Cauterization

(A) Schematics showing the asymmetric, symmetric upper, and symmetric lower patterns of whisker cauterization.

(B–D) VGlut2 staining (red) demonstrates the pattern of intact (filled arrowheads) and disrupted (asterisks) barrels resulting from (B) asymmetric, (C) symmetric upper, and (D) symmetric lower cauterization conditions. The presence of S1/S2 callosal projections in the contralateral hemisphere (GFP, right panels) demonstrate the conserved position (C and D, empty arrowhead) and density of fluorescence (quantified in E) of both symmetric treatments. Scale bar, 500 μm.

(E) Quantification of normalized fluorescence (f/fwm) across layers of symmetric upper (n = 7, gray) and symmetric lower (n = 6, green) cauterization conditions did not differ significantly (see Figures S5B–S5D for details; mean ± SEM).

(F and G) Representative examples of the S1/S2 callosal projection in (F) asymmetric and (G) symmetric cauterization conditions. Scale bar, 200 μm.

(H) Quantification of normalized fluorescence intensity across layers of asymmetric (n = 8), and symmetric (n = 13) conditions presented as a relative percentage of controls, showing a significant rescue of the symmetric condition as compared to the asymmetric condition (n = 7; symmetric treatments were pooled because they were not significantly different; mean ± SEM). U&L, upper and lower symmetric cauterizations. Student's t test: $**p < 0.01$. Mann-Whitney U test: $##p < 0.01$.

See also Figure S5 and Supplemental Experimental Procedures.
Figure options

Discussion

The innervation and stabilization of callosal projections is critical for the normal development of the brain and its full repertoire of functions. However, the mechanisms regulating callosal axon targeting are poorly understood. Here we have uncovered a process that contributes to interhemispheric axon guidance, whereby a spatially symmetric balance of early cortical activity between hemispheres is necessary for normal contralateral callosal targeting.

A seemingly similar study examined the effect of silencing the visual cortex with Kir2.1 electroporations at E15.5 and P2 (Mizuno et al., 2010). In their study, Mizuno et al. reported that unilateral, as well as bilateral, overexpression of Kir2.1 disrupted contralateral morphology of callosal axons labeled at P2 as compared to nonsilenced cells. However, these differing results do not necessarily imply an inconsistency with our study for three main reasons. First, as opposed to the somatosensory system, the visual system is not fully decussated; therefore, different mechanisms may affect callosal wiring in each system. Second, Mizuno et al., (2010) analyzed the terminal morphology of single

axons, whereas our study focused on contralateral projections from the entire barrel field. Third, we labeled and/or silenced callosal neurons at E15.5, while Mizuno et al. (2010) analyzed neurons electroporated at P2, possibly labeling a population of neurons guided by different developmental mechanisms.

Notably, our findings reveal that only callosal projections to the S1/S2 border, and not those to S1 or the Ins/PRh region, rely on balanced bilateral activity for appropriate targeting. This suggests that the function of balanced interhemispheric activity in regulating axon development in this circuit is region- and context specific. Moreover, it suggests that the development of distinct callosal projections arising from the same population of cells can be influenced by distinct factors. Although the functions of the S1/S2 and insular/perirhinal projections are not well understood, it is possible that their roles in brain function relate to their different targeting mechanisms used during development. For example, intact callosal connections to the S1/S2 region may be required for integrating lateralized somatosensory input (Shuler et al., 2001 and Shuler et al., 2002); therefore, it is possible that their development requires a balance of activity between brain areas that this projection will coordinate. The insular/perirhinal projection, on the other hand, has been poorly documented in the literature; although it is evident in classic tract-tracer and axon degeneration studies (Wise and Jones, 1976 and Ivy and Killackey, 1981), it was not described in studies using precise, layer-specific anterograde transport via in utero electroporation (Wang et al., 2007, Mizuno et al., 2007, Mizuno et al., 2010, Courchet et al., 2013 and Zhou et al., 2013). We speculate, however, that this projection may be involved in higher-order associative processing, possibly integrating functions from distinct cortical regions, and therefore may be insensitive to manipulations of a single sensory area.

Our results demonstrate that a spatial symmetry of sensory inputs is required for correct callosal development. This effect is not due to the disruption of inputs to any cortical region in particular, as the position and density of the S1/S2 projection were unchanged in bilaterally symmetric cauterizations of upper or lower rows of whiskers. Thus, the spatial symmetry of the manipulation holds more significance than the region of disruption. This result suggests that patterns of activity across the entire S1 (rather than on a cell-to-cell level) are a crucial regulator of callosal development. Future studies are required to fully understand this effect; however, we speculate that symmetric patterns of cortical activity between S1 hemispheres are detected by callosal axons during their targeting phase and spatially asymmetric manipulations of the sensory periphery impedes this process by altering the bilateral symmetry of activity in each S1 region.

The present findings reveal an additional mechanism by which early neural activity might affect brain wiring. We have shown that callosal axon targeting does not depend exclusively on intrinsic cell activity but rather on the relative contribution of activity between projecting cells and their target region. Seemingly similar scenarios have been demonstrated for a role of correlative activity between axon populations in axon targeting. For example, as axonal afferents from each eye converge on their targets, the relative contribution of

patterned activity from each eye determines the branching pattern and formation of cortical cytoarchitectural features, such as ocular dominance columns, in a competitive manner (Casagrande and Condo, 1988, Penn et al., 1998, Huberman et al., 2006, Ben Fredj et al., 2010, Ackman et al., 2012, Zhang et al., 2012 and Furman et al., 2013). Our study, however, reveals an entirely different process: rather than assessing the role of activity between axonal populations that compete for their targets, we have uncovered an instructive role of balanced activity between homologous regions in the development of their reciprocal connections. Furthermore, our data cannot be explained in the context of competition between thalamocortical and callosal axons, as we obtained similar results under conditions that disrupt the thalamic pathway (whisker cauterization) or leave it unaffected (Kir2.1 overexpression). Moreover, if thalamic axons were interacting competitively with callosal axons, then we would have expected an exuberance of callosal projections into the target region where thalamic input was disrupted; however, we found the opposite case (Figures S1C–S1E). Thus, a noncompetitive interaction, possibly involving a Hebbian-like matching of activity between hemispheres, is likely to mediate the development of the S1/S2 callosal projection.

Precisely how an interhemispheric balance of activity may direct callosal targeting remains open for future investigation. During the review of this article, Huang et al. (2013) published results indicating that bilateral sensory input may direct the target selection of callosal axons. While this finding supports our results, we additionally demonstrate that not only overall bilateral input but also a spatial symmetry of thalamic input and bilateral cortical activity are required for region-specific targeting of callosal axons. It has been previously shown that alteration of activity patterns can modulate growth cone responses to guidance cues (Ming et al., 2001, Hanson and Landmesser, 2004 and Nicol et al., 2007) as well as axon branch elaboration (Uesaka et al., 2005, Mizuno et al., 2010 and Courchet et al., 2013). Therefore, possible ways in which activity can regulate region-specific targeting of callosal projections may involve guidance decisions at the subplate and/or the branching and stabilization of arbors after innervating the cortical plate. Studies examining early postnatal cortical activity and axon guidance in vivo will be necessary to understand the processes underlying activity-dependent development of the corpus callosum.

In summary, we have demonstrated that a spatially symmetric interhemispheric balance of cortical activity during the first postnatal week is necessary for the correct targeting of callosal axons to the contralateral S1/S2 border. These results demonstrate a mechanism of axonal targeting based on a comparison of activity between two interconnected regions and reveal an important principle governing the contralateral targeting of callosal axons. Moreover, they demonstrate that alterations in the patterns of sensory and cortically driven activity may have profound effects on commissural axon targeting, with implications for understanding the etiology of brain wiring disorders.

Experimental Procedures

Animals and In Utero Electroporation

All animal procedures were approved by The University of Queensland Animal Ethics Committee. Time-mated CD1 dams underwent abdominal surgery (1–2 cm) at E15.5 to expose the uterine horns, and each embryo was injected with 0.5–1 μl of plasmid DNA (see Supplemental Experimental Procedures for details) in the lateral ventricle using a pulled glass pipette attached to a picospritzer (Parker Hannifin). Five 100-ms pulses at 30 V were delivered to S1 using 3 mm paddle electrodes (Nepagene) and an ECM 830 electroporator (BTX Harvard Apparatus). The uterine horns were placed back, and the dam was sutured and allowed to recover. Pups were screened, and those with fluorescent patches appropriately placed over S1 received whisker cauterization under ice anesthesia at P3. At P10, pups were perfused transcardially with 0.9% NaCl followed by 4% paraformaldehyde.

Immunohistochemistry and Microscopy

Coronal slices (50 μm) were mounted on slides and incubated for 3 hr in 5% v/v normal goat serum (NGS) and 0.2% Triton X-100 (TX100) in PBS (pH 7.4), followed by overnight incubation in 3% NGS and 0.2% TX100 in PBS with primary antibodies: rabbit anti-GFP (1:500; Invitrogen), chicken anti-GFP (1:750; Abcam), rabbit anti-vGlut2 (1:750; Synaptic Systems), and/or rabbit anti-DsRed (1:750; Clontech). After PBS washes, sections were then incubated for 3 hr with appropriate fluorescent secondary antibodies, stained with 0.1% DAPI (Invitrogen), washed, and coverslipped with ProLong Gold (Invitrogen). Only animals with cell bodies throughout L2/3 of S1 were selected for analysis (Figures S1N–S1Q; Supplemental Experimental Procedures) and two to three sections, spaced 200 μm apart, within the posteromedial barrel subfield were analyzed per animal. Images were obtained with an upright microscope (Axio Imager Z1, Zeiss) fitted with an AxioCam MRm camera and captured with AxioVision software using MosaicZ and/or ApoTome deconvolution (Zeiss). Densitometric quantification of green fluorescent protein (GFP)-positive axons was performed using a custom MATLAB program (MathWorks), similar to previous studies (Mizuno et al., 2007; see Figure S1R and Supplemental Experimental Procedures for details). Synaptophysin-positive puncta were counted over 20 to 50 μm sections of at least four representative axonal segments expressing both synaptophysin-GFP and Myr-tdTomato per animal.

Electrophysiology

Animals were decapitated, and their brains were sectioned coronally at 300 μm and kept in oxygenated (95% O2/5% CO2) artificial cerebrospinal fluid solution (118 mM NaCl, 2.5 mM KCl, 25 mM NaHCO3, 10 mM glucose, 1.3 mM MgCl2, 2.5 mM CaCl2, and 1.2 mM NaH2PO4). Whole-cell recordings were made from L2/3 cells of S1 of the electroporated hemisphere or the contralateral S1/S2 border. Only cells with a resting membrane potential more negative than −55 mV were included in this study. For Kir2.1 experiments, current-voltage relationship was determined by injecting 10 mV steps (−110 to 10 mV) at a holding potential of −30 mV. For optogenetic stimulation of callosal terminals, 5 ms 470 nm light pulses were delivered to the S1/S2 border contralateral to the electroporated hemisphere using an LED system (pE-2, CoolLed). An average of 10–15 light-evoked EPSCs (10 s interstimulation interval) was taken for evoked responses. The innervation rate was determined as the percentage of L2/3 neurons per

slice that had evoked EPSCs to optical stimulation of callosal terminals over the number of investigated neurons (two to seven neurons per slice, two to three slices per animal). Intrinsic firing properties were analyzed at current injections of 2-fold threshold firing (see Supplemental Experimental Procedures for details).

Author Contributions

L.J.R., R.S., and L.R.F. conceived the project and wrote the manuscript. R.S. and L.R.F. performed the majority of experiments and collected and analyzed the data. R.M. performed all electrophysiological experiments, analyzed the data, and contributed to writing the manuscript. L.A. wrote the software for image analysis and contributed to the analysis. P.S. and G.J.G. provided analytic tools and contributed to writing the manuscript.

Acknowledgments

We thank K. Deisseroth, A. Kriegstein, T. Saito, M. Stryker, and Y. Tagowa for providing DNA constructs; C. Wang, S. Liu, and J. Thomson for initial contributions to this project; L. Hammond for microscopy assistance; The University of Queensland Biological Resources and Queensland Brain Institute animal team for animal support; and R. Tweedale, P. Bartlett, J. Bertran-Gonzalez, and the Richards laboratory for input on the manuscript. This work was funded by National Health and Medical Research Council (NHMRC) project grants 1029975 and 1064174 (L.J.R.) 1043044 (G.J.G.) and by an Australian Research Council (ARC) Discovery project grant (P.S.). L.J.R. was supported by an NHMRC Principal Research Fellowship. P.S. was supported by an ARC Australian Professorial Fellowship. L.R.F. was supported by a University of Queensland Masters of Neuroscience scholarship and an Australian Postgraduate Award.

References

Ackman et al., 2012
J.B. Ackman, T.J. Burbridge, M.C. Crair
Retinal waves coordinate patterned activity throughout the developing visual system
Nature, 490 (2012), pp. 219–225

Ben Fredj et al., 2010
N. Ben Fredj, S. Hammond, H. Otsuna, C.B. Chien, J. Burrone, M.P. Meyer
Synaptic activity and activity-dependent competition regulates axon arbor maturation, growth arrest, and territory in the retinotectal projection
J. Neurosci., 30 (2010), pp. 10939–10951

Boyd et al., 1971
E.H. Boyd, D.N. Pandya, K.E. Bignall
Homotopic and nonhomotopic interhemispheric cortical projections in the squirrel monkey
Exp. Neurol., 32 (1971), pp. 256–274

Calford and Tweedale, 1990
M.B. Calford, R. Tweedale

Interhemispheric transfer of plasticity in the cerebral cortex
Science, 249 (1990), pp. 805–807

Casagrande and Condo, 1988
V.A. Casagrande, G.J. Condo
The effect of altered neuronal activity on the development of layers in the lateral geniculate nucleus
J. Neurosci., 8 (1988), pp. 395–416

Catania and Kaas, 2001
K.C. Catania, J.H. Kaas
Areal and callosal connections in the somatosensory cortex of the star-nosed mole
Somatosens. Mot. Res., 18 (2001), pp. 303–311

Cohan and Kater, 1986
C.S. Cohan, S.B. Kater
Suppression of neurite elongation and growth cone motility by electrical activity
Science, 232 (1986), pp. 1638–1640

Courchet et al., 2013
J. Courchet, T.L. Lewis Jr., S. Lee, V. Courchet, D.-Y. Liou, S. Aizawa, F. Polleux
Terminal axon branching is regulated by the LKB1-NUAK1 kinase pathway via presynaptic mitochondrial capture
Cell, 153 (2013), pp. 1510–1525

Ebner and Myers, 1962
F.F. Ebner, R.E. Myers
Corpus callosum and the interhemispheric transmission of tactual learning
J. Neurophysiol., 25 (1962), pp. 380–391

Fields et al., 1990
R.D. Fields, E.A. Neale, P.G. Nelson
Effects of patterned electrical activity on neurite outgrowth from mouse sensory neurons
J. Neurosci., 10 (1990), pp. 2950–2964

Fox, 1992
K. Fox
A critical period for experience-dependent synaptic plasticity in rat barrel cortex
J. Neurosci., 12 (1992), pp. 1826–1838

Furman et al., 2013
M. Furman, H.P. Xu, M.C. Crair
Competition driven by retinal waves promotes morphological and functional synaptic development of neurons in the superior colliculus
J. Neurophysiol., 110 (2013), pp. 1441–1454

Garaschuk et al., 2000
O. Garaschuk, J. Linn, J. Eilers, A. Konnerth
Large-scale oscillatory calcium waves in the immature cortex
Nat. Neurosci., 3 (2000), pp. 452–459

Gazzaniga, 2000
M.S. Gazzaniga
Cerebral specialization and interhemispheric communication: does the corpus callosum enable the human condition?
Brain, 123 (2000), pp. 1293–1326

Goldberg et al., 2002
J.L. Goldberg, J.S. Espinosa, Y. Xu, N. Davidson, G.T.A. Kovacs, B.A. Barres
Retinal ganglion cells do not extend axons by default: promotion by neurotrophic signaling and electrical activity
Neuron, 33 (2002), pp. 689–702

Hanson and Landmesser, 2004
M.G. Hanson, L.T. Landmesser
Normal patterns of spontaneous activity are required for correct motor axon guidance and the expression of specific guidance molecules
Neuron, 43 (2004), pp. 687–701

Harwell et al., 2012
C.C. Harwell, P.R.L. Parker, S.M. Gee, A. Okada, S.K. McConnell, A.C. Kreitzer, A.R. Kriegstein
Sonic hedgehog expression in corticofugal projection neurons directs cortical microcircuit formation
Neuron, 73 (2012), pp. 1116–1126

Huang et al., 2013
Y. Huang, N.N. Song, W. Lan, Q. Zhang, L. Zhang, L. Zhang, L. Hu, J.Y. Chen, C.J. Zhao, L. Li, et al.
Sensory input is required for callosal axon targeting in the somatosensory cortex
Mol. Brain, 6 (2013), p. 53

Huberman et al., 2006
A.D. Huberman, C.M. Speer, B. Chapman
Spontaneous retinal activity mediates development of ocular dominance columns and binocular receptive fields in v1
Neuron, 52 (2006), pp. 247–254

Innocenti and Fiore, 1976
G.M. Innocenti, L. Fiore
Morphological correlates of visual field transformation in the corpus callosum
Neurosci. Lett., 2 (1976), pp. 245–252

Innocenti and Frost, 1979
G.M. Innocenti, D.O. Frost

Effects of visual experience on the maturation of the efferent system to the corpus callosum
Nature, 280 (1979), pp. 231–234

Ivy and Killackey, 1981
G.O. Ivy, H.P. Killackey
The ontogeny of the distribution of callosal projection neurons in the rat parietal cortex
J. Comp. Neurol., 195 (1981), pp. 367–389

Katz and Shatz, 1996
L.C. Katz, C.J. Shatz
Synaptic activity and the construction of cortical circuits
Science, 274 (1996), pp. 1133–1138

Khazipov and Luhmann, 2006
R. Khazipov, H.J. Luhmann
Early patterns of electrical activity in the developing cerebral cortex of humans and rodents
Trends Neurosci., 29 (2006), pp. 414–418

Khazipov et al., 2013
R. Khazipov, M. Minlebaev, G. Valeeva
Early gamma oscillations
Neuroscience, 250 (2013), pp. 240–252

Koralek and Killackey, 1990
K.A. Koralek, H.P. Killackey
Callosal projections in rat somatosensory cortex are altered by early removal of afferent input
Proc. Natl. Acad. Sci. USA, 87 (1990), pp. 1396–1400

Kretz and Rager, 1990
R. Kretz, G. Rager
Reciprocal heterotopic callosal connections between the two striate areas in Tupaia
Exp. Brain Res., 82 (1990), pp. 271–278

Krubitzer et al., 1998
L. Krubitzer, J.C. Clarey, R. Tweedale, M.B. Calford
Interhemispheric connections of somatosensory cortex in the flying fox
J. Comp. Neurol., 402 (1998), pp. 538–559

Ming et al., 2001
G. Ming, J. Henley, M. Tessier-Lavigne, H. Song, M. Poo
Electrical activity modulates growth cone guidance by diffusible factors
Neuron, 29 (2001), pp. 441–452

Minlebaev et al., 2011

M. Minlebaev, M. Colonnese, T. Tsintsadze, A. Sirota, R. Khazipov
Early γ oscillations synchronize developing thalamus and cortex
Science, 334 (2011), pp. 226–229

Mire et al., 2012 E. Mire, C. Mezzera, E. Leyva-Díaz, A.V. Paternain, P. Squarzoni, L. Bluy, M. Castillo-Paterna, M.J. López, S. Peregrín, M. Tessier-Lavigne, et al.
Spontaneous activity regulates Robo1 transcription to mediate a switch in thalamocortical axon growth
Nat. Neurosci., 15 (2012), pp. 1134–1143

Mizuno et al., 2007 H. Mizuno, T. Hirano, Y. Tagawa
Evidence for activity-dependent cortical wiring: formation of interhemispheric connections in neonatal mouse visual cortex requires projection neuron activity
J. Neurosci., 27 (2007), pp. 6760–6770

Mizuno et al., 2010 H. Mizuno, T. Hirano, Y. Tagawa
Pre-synaptic and post-synaptic neuronal activity supports the axon development of callosal projection neurons during different post-natal periods in the mouse cerebral cortex
Eur. J. Neurosci., 31 (2010), pp. 410–424

Nicol et al., 2007 X. Nicol, S. Voyatzis, A. Muzerelle, N. Narboux-Nême, T.C. Südhof, R. Miles, P. Gaspar
cAMP oscillations and retinal activity are permissive for ephrin signaling during the establishment of the retinotopic map
Nat. Neurosci., 10 (2007), pp. 340–347

Olavarria et al., 1987 J. Olavarria, R. Malach, R.C. Van Sluyters
Development of visual callosal connections in neonatally enucleated rats
J. Comp. Neurol., 260 (1987), pp. 321–348

Penn et al., 1998 A.A. Penn, P.A. Riquelme, M.B. Feller, C.J. Shatz
Competition in retinogeniculate patterning driven by spontaneous activity
Science, 279 (1998), pp. 2108–2112

Petreanu et al., 2007 L. Petreanu, D. Huber, A. Sobczyk, K. Svoboda
Channelrhodopsin-2-assisted circuit mapping of long-range callosal projections
Nat. Neurosci., 10 (2007), pp. 663–668

Shuler et al., 2001 M.G. Shuler, D.J. Krupa, M.A.L. Nicolelis
Bilateral integration of whisker information in the primary somatosensory cortex of rat
J. Neurosci., 21 (2001), pp. 5251–5261

Shuler et al., 2002 M.G. Shuler, D.J. Krupa, M.A.L. Nicolelis
Integration of bilateral whisker stimuli in rats: role of the whisker barrel cortices
Cereb. Cortex, 12 (2002), pp. 86–97

Spitzer, 2006 N.C. Spitzer

Electrical activity in early neuronal development
Nature, 444 (2006), pp. 707–712

Tang et al., 2003 F. Tang, E.W. Dent, K. Kalil
Spontaneous calcium transients in developing cortical neurons regulate axon outgrowth
J. Neurosci., 23 (2003), pp. 927–936

Uesaka et al., 2005 N. Uesaka, S. Hirai, T. Maruyama, E.S. Ruthazer, N. Yamamoto
Activity dependence of cortical axon branch formation: a morphological and electrophysiological study using organotypic slice cultures
J. Neurosci., 25 (2005), pp. 1–9

Wang et al., 2007 C.L. Wang, L. Zhang, Y. Zhou, J. Zhou, X.J. Yang, S.M. Duan, Z.Q. Xiong, Y.Q. Ding
Activity-dependent development of callosal projections in the somatosensory cortex
J. Neurosci., 27 (2007), pp. 11334–11342

Wise and Jones, 1976 S.P. Wise, E.G. Jones
The organization and postnatal development of the commissural projection of the rat somatic sensory cortex
J. Comp. Neurol., 168 (1976), pp. 313–343

Wise and Jones, 1978 S.P. Wise, E.G. Jones
Developmental studies of thalamocortical and commissural connections in the rat somatic sensory cortex
J. Comp. Neurol., 178 (1978), pp. 187–208

Woolsey and Van der Loos, 1970 T.A. Woolsey, H. Van der Loos
The structural organization of layer IV in the somatosensory region (SI) of mouse cerebral cortex. The description of a cortical field composed of discrete cytoarchitectonic units
Brain Res., 17 (1970), pp. 205–242

Yamada et al., 2010 A. Yamada, N. Uesaka, Y. Hayano, T. Tabata, M. Kano, N. Yamamoto
Role of pre- and postsynaptic activity in thalamocortical axon branching
Proc. Natl. Acad. Sci. USA, 107 (2010), pp. 7562–7567

Yang et al., 2009 J.W. Yang, I.L. Hanganu-Opatz, J.J. Sun, H.J. Luhmann
Three patterns of oscillatory activity differentially synchronize developing neocortical networks in vivo
J. Neurosci., 29 (2009), pp. 9011–9025

Yorke and Caviness, 1975 C.H. Yorke Jr., V.S. Caviness Jr.
Interhemispheric neocortical connections of the corpus callosum in the normal mouse: a study based on anterograde and retrograde methods
J. Comp. Neurol., 164 (1975), pp. 233–245

Zhang et al., 1998 L.I. Zhang, H.W. Tao, C.E. Holt, W.A. Harris, M. Poo
A critical window for cooperation and competition among developing retinotectal synapses
Nature, 395 (1998), pp. 37–44

Zhang et al., 2012 J. Zhang, J.B. Ackman, H.P. Xu, M.C. Crair
Visual map development depends on the temporal pattern of binocular activity in mice
Nat. Neurosci., 15 (2012), pp. 298–307

Zhou et al., 2013 J. Zhou, Y. Wen, L. She, Y.N. Sui, L. Liu, L.J. Richards, M.M. Poo
Axon position within the corpus callosum determines contralateral cortical projection
Proc. Natl. Acad. Sci. USA, 110 (2013), pp. E2714–E2723